Journal of Food Engineering 263 (2019) 288–298

Contents lists available at ScienceDirect

Journal of Food Engineering

journal homepage: www.elsevier.com/locate/jfoodeng

Tomato volume and mass estimation using computer vision and machine learning algorithms: Cherry tomato model

Innocent Nyalala[a], Cedric Okinda[a], Luke Nyalala[b], Nelson Makange[a], Qi Chao[a], Liu Chao[a], Khurram Yousaf[a], Kunjie Chen[a,*]

[a] College of Engineering, Nanjing Agricultural University, Nanjing, 210031, China
[b] Department of Computer Science, Cornell University, Ithaca, NY, 14853-7501, USA

ARTICLE INFO

Keywords:
Computer vision
Cherry tomato
Mass estimation
Machine learning algorithms
Volume estimation
Fruit sorting and grading

ABSTRACT

A prediction method of mass and volume of cherry tomato based on a computer vision system and machine learning algorithms were introduced in this study. The relation between tomato mass and volume was established as $M = 1.312V^{0.9551}$, and was used to estimate mass on a test dataset at an R^2 of 0.9824 and RMSE of 15.84g. Depth images of tomatoes at different orientations were acquired and features extracted by image processing techniques. Five regression prediction models based on 2D and 3D image features were developed. The RBF-SVM outperformed all explored models with an accuracy of 0.9706 (only 2D features) and 0.9694 (all features) in mass and volume estimation respectively. The model predicted mass or volume can then be applied to the established mass-volume power function. This introduced system can be applied as a non-destructive, accurate and consistent technique to in-line sorting and grading of cherry tomatoes based on mass, volume or density.

1. Introduction

Tomato (*Solanum lycopersicum*) is one of the globally highly produced and consumed agricultural product (Van de Poel et al., 2012; Wan et al., 2018; Wei et al., 2016). According to FAOSTAT (2017), global production of tomatoes in 2017 was 182 million tons. Over the years, tomatoes have become an essential vegetable because it is rich in minerals, and anti-oxidants for the human diet (Rizzolo et al., 2010). Additionally, consumption of tomato has been associated with decreased risk of some cancers, osteoporosis, and cardiovascular disease, since it is also rich in fiber and vitamins A and C (Chang et al., 2006; Kumar et al., 2012; Saad et al., 2016; Takeoka et al., 2001; Wan et al., 2018).

With largescale production, arises the challenge of grading and sorting in the supply chain management. Geometrical attributes, size, and dimensions are regarded as crucial factors in the grading of raw agricultural produce (Khojastehnazhand et al., 2010a). Appearance is the primary quality feature considered by consumers despite the inherent quality of a fruit and vegetable being essential (Arendse et al., 2018). It is the external quality that significantly impacts market prices and consumers. The shape, color, size, texture, shelf life (maturity) and visual flaws are mainly inspected to evaluate the outside quality of ripe fruits (Naik and Patel, 2017). These factors also affect storage and transportation options, which directly influences the sales and marketing of the products by food industries (Du and Sun, 2006b).

Tomatoes have traditionally been classified by manual sorting according to their physiological maturity (Van de Poel et al., 2012). However, this technique is time-consuming, expensive, subjective, and inaccurate (Ehsani et al., 2016; Satpute and Jagdale, 2016). Currently, several computer vision techniques have been introduced and are increasingly becoming vital in fruit and vegetable sorting (Chen et al., 2002). These systems offer many advantages, such as consistency and uniformity in grading, speed, and accuracy in sorting. Moreover, they have a high success rate and non-destructive methods (Gül and Özdemir, 2017).

Computer vision systems in fruits and vegetable sorting mainly focus on features such as maturity, color, defects, and size of the fruit (Jadhav et al., 2019). Size determination is an appropriate step in fresh fruit post-harvest operations (Concha-Meyer et al., 2018). The size of a fruit corresponds to its volume, surface area, and mass (Omid et al., 2010). Thus, these variables can be used as essential descriptors in sorting and grading of fruits (Moreda et al., 2009). Volume computation is essential for density-based sorting of fruits and optimization of space in volume based packaging (Jadhav et al., 2019; Moreda et al., 2009).

* Corresponding author. College of Engineering, Nanjing Agricultural University, Nanjing, Jiangsu, 210031, PR China.
E-mail address: kunjiechen@njau.edu.cn (K. Chen).

https://doi.org/10.1016/j.jfoodeng.2019.07.012
Received 23 April 2019; Received in revised form 12 July 2019; Accepted 12 July 2019
Available online 14 July 2019

Abbreviations

M	Mass	TB	Terabyte
V	Volume	ROI	Region of Interest
2D	2 dimensional	*A*	Area
3D	3 dimensional	*P*	Perimeter
RBF	Radial basis function	*E*	Eccentricity
SVM	Support Vector Machine	λ_1	Major-Axis Length
g	Grams	λ_2	Minor-Axis Length
WDM	Water displacement method	λ_2	Radial Distance
FOV	Field of View	*S*	Surface Area
TOF	Time of Flight	ANN	Artificial Neural Network
USB	Universal Serial Bus	*M1*	Model 1, based on only 2D image features
CPU	Central Processing Unit	*M2*	Model 2, based on only 3D image features
GHz	Gigahertz	*M3*	Model 3, based on both 2D and 3D image features
GB	Gigabyte	R^2	Coefficient of determination
PC	Personal Computer	RMSE	Root Mean Square Error
SDK	Software Development Kit	ml	Millimeter
fpm	Frames per Minute	SSE	The Square Sum of the Estimate
		R^2 adj	R-Squared Adjusted for the degree of freedom
		RGB	Color model of Red, Green, and blue

Suppose the density of a product remains constant, its volume can help ascertain its mass (Duzyaman and Duzyaman, 2005; Ioana et al., 2007). When the volume is combined with the mass, the average density can be established, which is vital in detecting hidden defects such as internal damage and frost damage. The average density can additionally provide biomass, water content, and consistency information of agricultural produce. Alternatively, if the fruit densities are assumed to be almost constant, then the system can estimate fruit mass from the volume, replacing the need for a weighing device (Chopin et al., 2017; Iqbal et al., 2011). Several kinds of literature have reported having developed systems that could determine volume, surface area, and mass information of agricultural food products based on computer vision techniques (Costa et al., 2011; Eifert et al., 2006; Khojastehnazhand et al., 2010a, 2010b; Lee et al., 2002; Li et al., 2002; Moreda et al., 2009; Omid et al., 2010; Schulze et al., 2015; Wang et al., 2017; Ziaratban et al., 2017).

A study by Siswantoro et al. (2013) classified food products into axys-symmetric shaped and irregularly shaped objects; the study established that a product could be regarded as an axys-symmetric object if its cross-sections are circular while perpendicular to its major axis. Additionally, Sabliov et al. (2002); Wang and Nguang (2007) concluded that surface area and volume of axys-symmetric products such as eggs, peaches, limes, and lemon, can be estimated by capturing one image from a fixed projection and dividing the image into a set of cylindrical objects. Furthermore, Vivek Venkatesh et al. (2015) determined the relationship between the mass of axys-symmetric fruits (oranges, apples, lemons, and sweet-limes) and their estimated volume using image processing-based techniques. Likewise, Koc (2007); Rashidi and Gholami (2008) estimated the volume of watermelons and kiwi fruits by ellipsoid approximation techniques. Du and Sun (2006a) developed an automatic method for estimating volume and surface area of ham using an image partitioning and spherical modeling methodology.

In the sorting of irregular shaped agricultural products, Siswantoro et al. (2013) suggested the use of 3D reconstruction using silhouettes from multiple views of the object for volume estimation. Thus, the

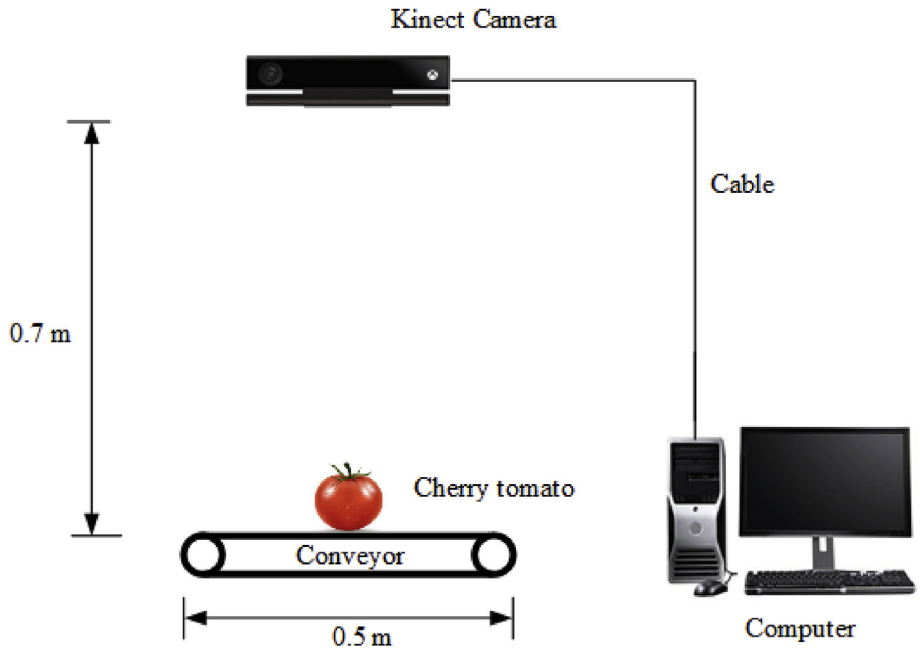

Fig. 1. Experimental setup and image acquisition system.'

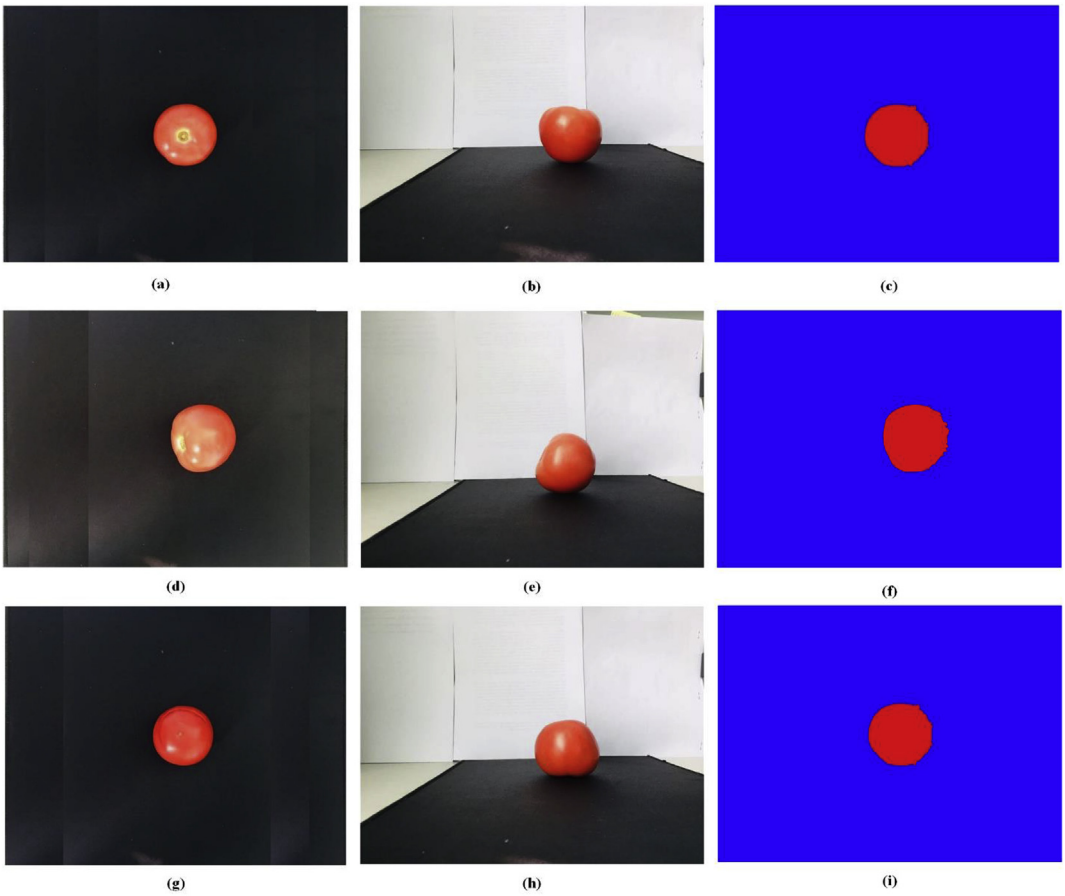

Fig. 2. Tomato image acquisition at different orientations, (a, b and c) overhead RGB, side, RGB, and a depth image of a tomato in the first orientation. (d, e and f) overhead RGB, side RGB, and a depth image of a tomato in the second orientation. (g, h and i). overhead RGB, side RGB, and a depth image of a tomato in the third orientation.

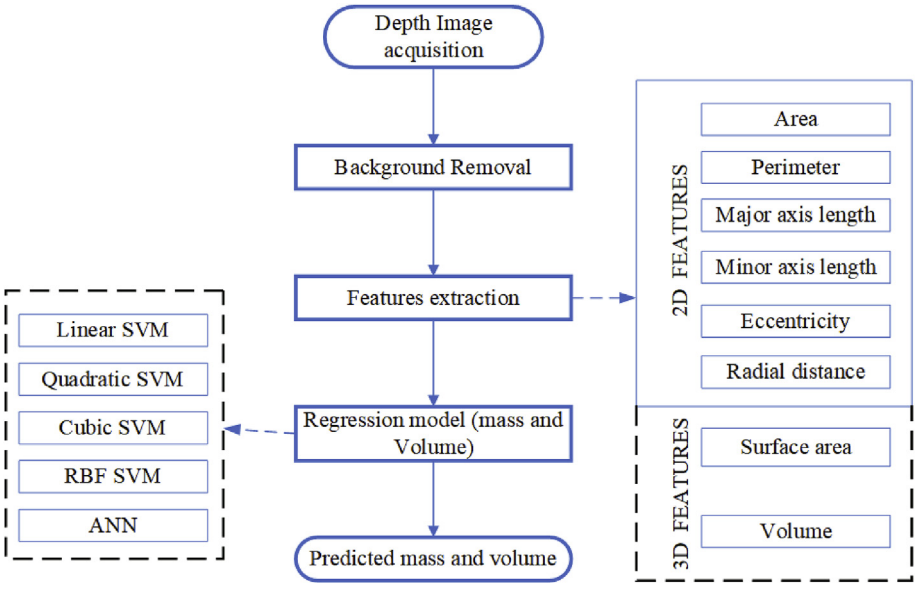

Fig. 3. The algorithmic flow of the proposed system.

volume can be measured by counting the number of voxels in the reconstructed 3D object or by a mathematical model. This technique was successfully applied by Jadhav et al., (2019) to estimate the volume of apple, orange, mango, strawberry, and pomegranate fruits using volumetric 3D reconstruction in multiple cameras fruit grading system. Lee et al. (2006) designed a computer vision system that could measure volume using multiple silhouettes based on a mathematical model for volume approximation from a 3D wireframe model, which used images acquired from multiple views of a rotating irregular shaped object using a turntable in a fixed, regular interval. Also, Ireri et al., (2018)

Table 1
Parameters of the developed regression models.

Classifier parameters	*M1*		*M2*		*M3*	
SVM kernel parameters	Scale	degree	Scale	degree	Scale	degree
Linear						
Prediction of *V*	0.428	–	0.486	–	0.524	–
Prediction of *M*	0.495	–	0.541	–	0.579	–
Quadratic						
Prediction of *V*	0.431	2	0.516	2	0.610	2
Prediction of *M*	0.510	2	0.620	2	0.697	2
Cubic						
Prediction of *V*	0.396	3	0.424	3	0.503	3
Prediction of *M*	0.467	3	0.578	3	0.636	3
RBF						
Prediction of *V*	0.520	–	0.670	–	0.795	–
Prediction of *M*	0.620	–	0.696	–	0.753	–
Bayesian-ANN topology	6-10-1		2-10-1		8-10-1	

Table 2
Mass estimation using the power model.

Measured *M* (g)	Estimated *M* (g)	Error (g)	Relative Error (%)
129.8	136.572	6.772	5.217
509.6	506.221	−3.378	0.662
459.5	463.039	3.539	0.771
349.3	357.813	8.513	2.437
279.2	287.674	8.474	3.035
289.0	290.105	1.105	0.382
247.8	246.191	−1.608	0.648
397.9	396.705	−1.194	0.304
217.5	225.427	7.927	3.645
227.3	221.638	−5.661	2.491

Average Relative Error (n = 50) = 4.600%.

Table 3
Performance evaluation of the three models used for mass and volume estimation.

Regression Models	*M1*		*M2*		*M3*	
	Mass	Volume	Mass	Volume	Mass	Volume
Linear SVM	0.9255	0.9346	0.9263	0.9013	0.9392	0.9285
Quadratic SVM	0.9499	0.9362	0.9250	0.9011	0.9579	0.9497
Cubic SVM	0.9640	0.9367	0.9247	0.9141	0.9598	0.9694
RBF-SVM	0.9706	0.9420	0.9263	0.9226	0.9622	0.9694
Bayesian-ANN	0.9644	0.9663	0.9340	0.9282	0.9681	0.9595

introduced a low-cost tomato sorter using a monochrome camera.

Computer vision techniques for estimation of volume and mass of axys-symmetric fruits are an essential aspect towards improved post-harvest technologies. This paper outlines an investigation of the inter-relation between tomato mass and volume and developed models to predict the two variables based on 2D and 3D image features. The correlation of the predicted variables was compared to those of the real mass and volume. Several tomato grading and sorting systems already exist based on computer vision techniques (El-Bendary et al., 2015; El Hariri et al., 2014b; Semary et al., 2015). However, this study presents a novel approach based on the combined 2D and 3D image system and develops a comparative approach between the introduced system and solely 2D and 3D tomato sorting systems.

The primary objective of this study was to develop a computer vision system for the estimation of mass and volume of cherry tomatoes. The specific objectives were (1) to develop an efficient depth image processing algorithm, (2) to develop both 2D and 3D feature extraction algorithm, (3) to develop mass and volume estimation regression models based on the extracted features, and (4) to investigate the relationship between tomato mass and volume.

2. Materials and methods

2.1. Experimental setup and data collection

Experiments were conducted between September and December 2018 at Nanjing Agricultural University, College of Engineering Pukou, Nanjing, Jiangsu Province, China. A total of 300 fresh cherry tomatoes of various sizes were purchased from a local market in Pukou district. Cherry tomato is the most famous tomato fruit variety grown in east China and was readily available in the market during the experimental duration of this study. The tomatoes were ripe and free from any visible injuries and defects. During the experiment, each tomato was labeled, weighed by a calibrated electronic scale (YP10001 model, Shanghai 00000271 Instruments Company) having an accuracy of ± 0.1 g and volume determined by water displacement method (WDM) (Mohsenin, 1970).

2.2. Image acquisition system

The imaging system consisted of a 3D Kinect sensor (Model Kinect 2.0, Microsoft, Seattle, WA, USA), mounted on a metal stand 0.7 m

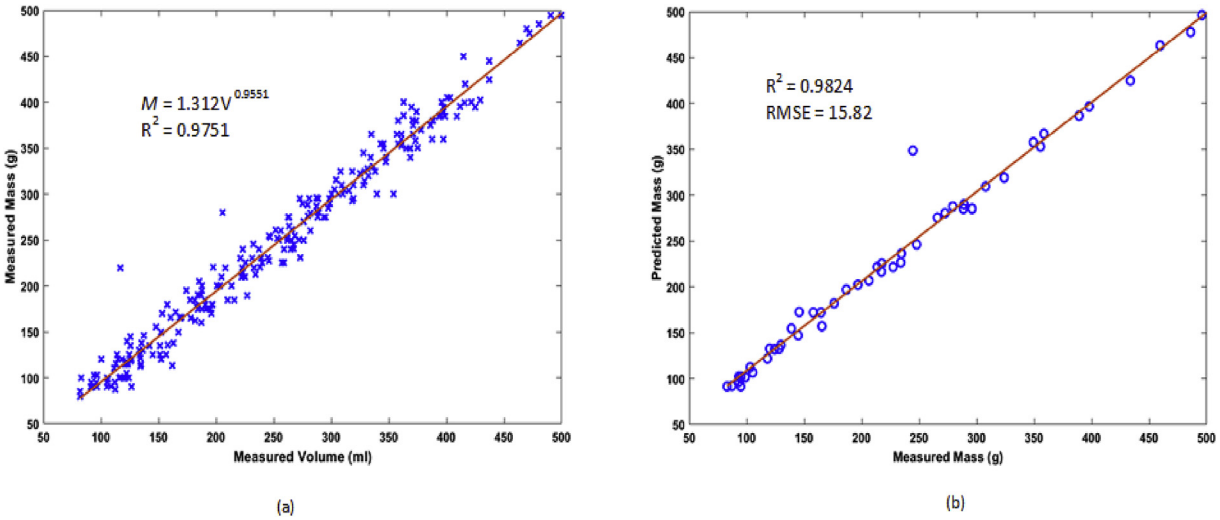

Fig. 4. (a) Scatter plot of the relationship between measured volume and measured mass (b). Scatter plot of the relationship between measured mass and predicted mass based on the power model.

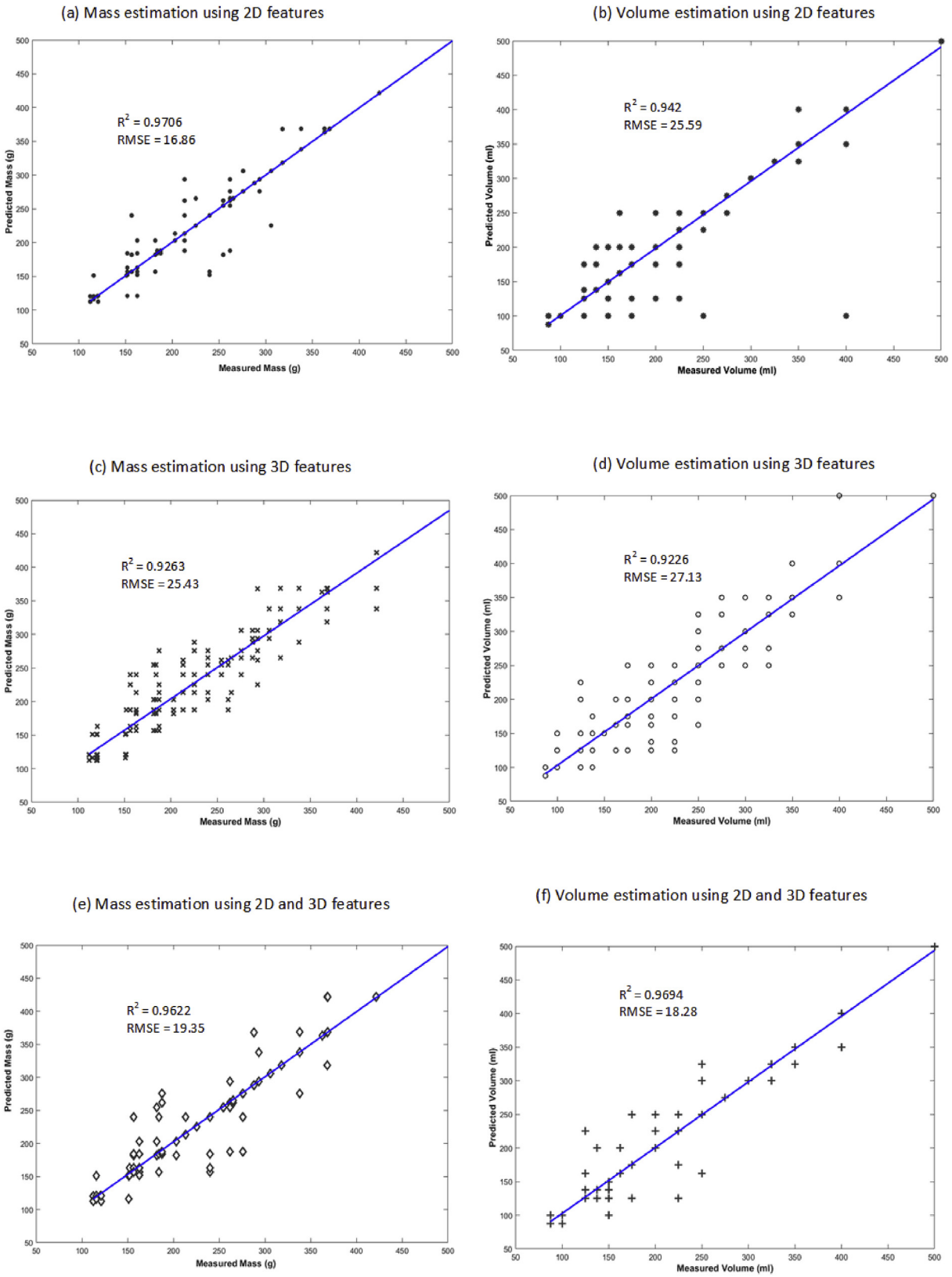

Fig. 5. Scatter plot of the correlation between predicted V and M with the measured V and. M of the three models (M1, M2, and M3) with the RBF-SVM.

(within the field of view (FOV)) perpendicularly above a conveyor belt (scanning stage) as shown in Fig. 1. The Kinect depth camera was used in this study because it can provide 3D information needed for volume computation, and it is the most efficient and reliable low-cost TOF (Time-of-flight) camera currently available in the market. The infrared (IR) depth sensor also provides faster high-quality depth estimation, ease of image segmentation, has proper manufactured calibration and it is invariant to ambient visible light conditions compared to visible light-based sensors (Andersen et al., 2012; Corti et al., 2016; Gonzalez-Jorge et al., 2015; Nguyen et al., 2018; Okinda et al., 2018). The Kinect

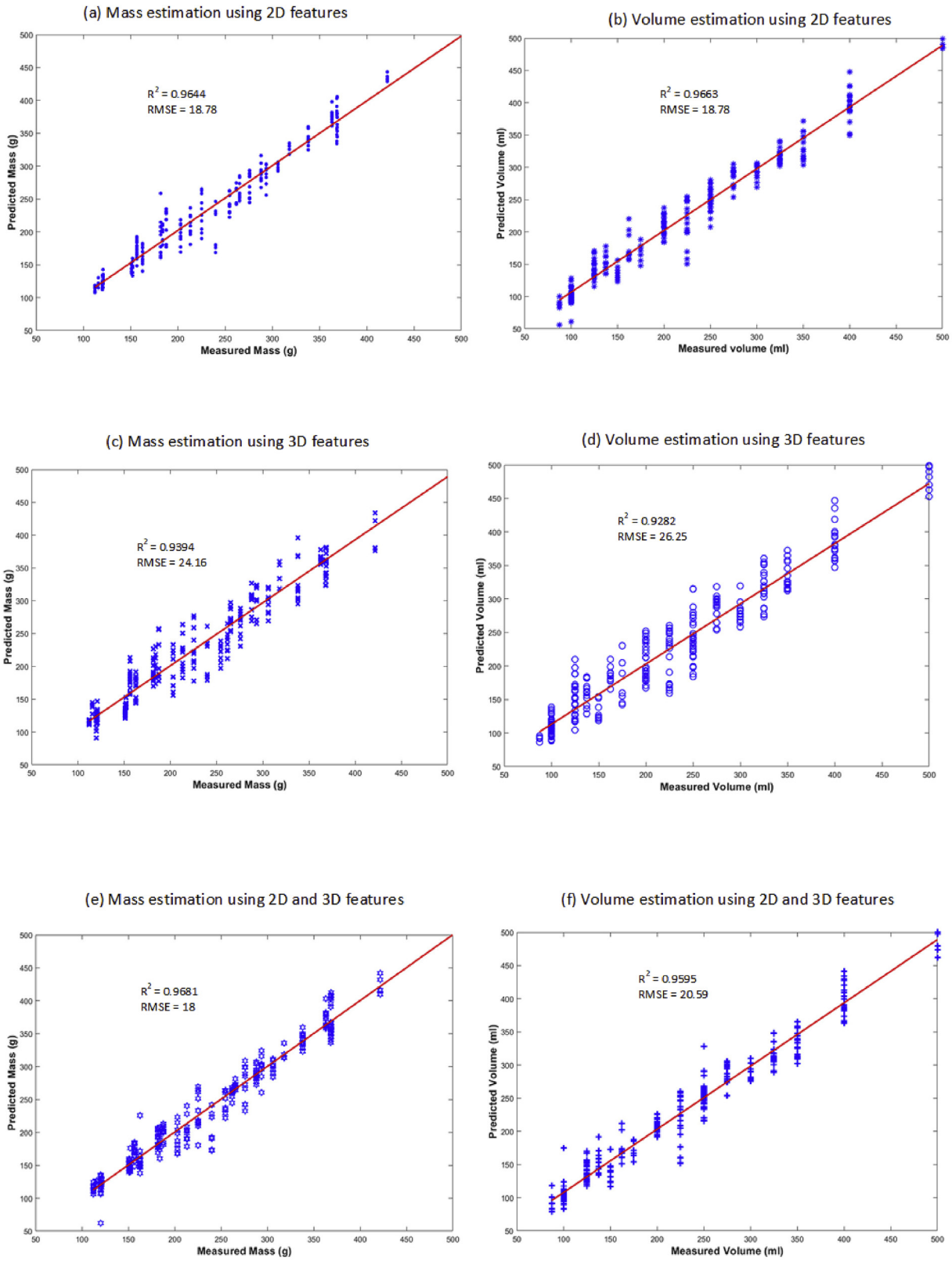

Fig. 6. Scatter plot of the correlation between predicted V and M with the measured V and. M of the three models (M1, M2, and M3) with Bayesian-ANN.

camera was connected via a USB port to an Intel i7- 4700HQ CPU, 2.4 GHz, 16 GB physical memory (Intel, Santa Clara, CA, USA), Microsoft Windows 10 PC installed with the Kinect for Windows Software Development Kit (SDK). Images were acquired from the Kinect camera using MATLAB R2019a (The MathWorks Inc., Natick, MA) software with the image acquisition Toolkit (IAT). Depth images (424 × 512 pixels) were acquired at 10 fpm and transferred to a 1 TB hard drive for subsequent analysis.

For each tomato, a total of 9 images were captured, 3 for each orientation and position on the scanning stage. The first orientation was

Table 4
Descriptive statistics based on measured tomato mass and volume ($n = 300$).

Measured Mass		Measured Volume	
Descriptive statistic	Value (g)	Descriptive statistic	Value (ml)
Mean	249.04	Mean	244.88
Standard Error	6.38	Standard Error	6.44
Median	242.30	Median	231.00
Standard Deviation	110.45	Standard Deviation	111.50
Sample Variance	12198.21	Sample Variance	12431.33
Skewness	0.38	Skewness	0.39
Range	430.70	Range	430.50
Minimum	81.90	Minimum	80.00
Maximum	512.60	Maximum	510.50

with the stalk scar facing upward. Secondly, stalk scar facing downward, and lastly, the longitudinal axes of the stalk scar parallel to the scanning stage surface, as shown in Fig. 2.

2.3. Image processing and feature extraction algorithm

These algorithms aimed at extracting image properties to be used to develop correlations to tomato mass and volume. The extraction of these feature variables was performed on a processed depth image. Fig. 3 presents the algorithmic flow diagram of the proposed system.

2.3.1. Image pre-processing

Processing of raw depth image data was performed according to the following procedure:

1. Background removal was performed using the image subtraction technique, as shown in Eq. (1) (Li et al., 2002).

$$g(x, y) = \begin{cases} 0, & if|f(x, y) - b(x - y)| \le T \\ f(x, y) & otherwise \end{cases} \quad (1)$$

where $g(x, y)$ is the resultant image after its background has been removed, $f(x, y)$ is the original image, $b(x, y)$ is the background image, and T is the threshold.

2. Distance thresholding was carried out based on distance intensities of the depth image to obtain the region of interest (ROI) after setting to remain with maximum and minimum thresholds (Jana, 2012).
3. Smoothening was done on the resultant depth image using the Gaussian kernel filter (15 × 15 pixels zero mean) (Eq. (2)) then morphological opening by a disk structural element of size 9 pixels to remove small holes and obtain a clear depth image (Eq. (3)).
4. Binarization was then implemented to convert the depth image into a binary image using Otsu's method (Otsu, 1979).

$$h(x, y) = m[g(x, y)] \quad (2)$$

where $h(x, y) = h$ is the resultant filtered image, and $m = \left(\frac{1}{2\pi\sigma^2} e^{-\frac{1}{2}\left(\frac{e^2+f^2}{\sigma^2}\right)} \right)$ is the Gaussian filter kernel.

$$h.\ Tn = (g \oplus Tn)\,\Theta Tn = \cup\{((Tn)_p|(Tn)_p)\} \quad (3)$$

where Tn is the structural element, $(Tn)_p$ is the translation of Tn by a point p.

2.4. Feature extraction

These features are categorized depending on the underlying space from which they were extracted such 2D and 3D image features. In order to obtain the best performance, it is necessary to combine these multidimensional features (Mathiassen et al., 2011). In this study, a combination of six 2D and two 3D features was used for estimating the volume and mass of the tomatoes.

2.4.1. 2D features

Projected area (A), perimeter (P), eccentricity (E), major-axis length (λ_1), minor-axis length (λ_2), and radial distance (D) were used as 2D features. The area has been widely used as a feature for volume and mass estimation in fruits (Omid et al., 2010). A is simply the area which the tomato takes up when projected onto the image plane or the actual number of pixels inside an object. The A is defined by Eq. 4

$$A = \frac{1}{2} \sum_{n-1}^{N-1} (y_{n+1}x_n - x_{n+1}y_n) \quad (4)$$

This formula has been derived from the *Green's Theorem* which relates a 2D integral $\iint_{ROI}$ on a ROI with a line integral $\oint_{\partial ROI}$ on the closed boundary of the ROI (Morrey, 2009).

The P is the distance around the boundary of the object; it was computed by counting the number of pixels in the closed contour. Consider an image shape having N vertices: $C = \{(x_n, y_n)\}$, with $n = 1, ..., N$, and $(x_1, y_1) = (x_N, y_N)$, then P is defined by Eq. (5).

$$P = \sum_{n-1}^{N-1} (x_{n+1}, y_{n+1}) - (x_n, y_n) \quad (5)$$

E is a ratio of λ_1 and λ_2 when an ellipse is fitted on an image; a more circular object shape will have a lower eccentricity. E can be computed using the principal axes method according to Eq. (6).

$$E = \frac{\lambda_1}{\lambda_2} \quad (6)$$

The λ_1 is the pixel distance between the major-axis endpoints and is given by Eq. (7).

$$\lambda_1 = \sqrt{(X_2 - X_1)^2 + (Y_2 - Y_1)^2} \quad (7)$$

where the major-axis endpoint coordinates are described by (X_1, Y_1) and (X_2, Y_2). The result is the Euclidian distance between the two points.

The λ_2 is the pixel distance between the minor-axis endpoints and is given by Eq. (8).

$$\lambda_2 = \sqrt{(M_2 - M_1)^2 + (N_2 - N_1)^2} \quad (8)$$

where the minor-axis endpoint coordinates are described by (M_2, N_2) and (M_1, N_1). The result is the Euclidian distance between the two points.

Table 5
Summary of performance evaluation of the Bayesian-ANN model, where SSE is the square sum error of the estimate, R^2 is the coefficient of determination, R^2 adj. is R-squared adjusted for the degree of freedom, and RMSE is the root mean square error.

	M1		*M2*		*M3*	
	Mass	Volume	Mass	Volume	Mass	Volume
SSE	1.012e+05	1.009e+05	1.676e+05	1.971e+05	9.269e+04	1.212e+05
R^2	0.9644	0.9663	0.9394	0.9282	0.9681	0.9595
R^2 adj	0.9643	0.9661	0.9392	0.928	0.9679	0.9593
RMSE	18.78	18.78	24.16	26.25	18	20.59

Table 6
Summary of performance evaluation of the RBF-SVM model, where SSE is the square sum error of the estimate, R^2 is the coefficient of determination, R^2 adj. is R-squared adjusted for the degree of freedom, and RMSE is the root mean square error.

	M1		*M2*		*M3*	
	Mass	Volume	Mass	Volume	Mass	Volume
SSE	8.125e+04	1.873e+05	1.85e+05	2.097e+05	1.071e+05	9.555e+04
R^2	0.9706	0.942	0.9263	0.9226	0.9622	0.9694
R^2 adj	0.9705	0.9418	0.9261	0.9223	0.9621	0.9693
RMSE	16.86	25.59	25.43	27.13	19.35	18.28

Table 7
Comparison between measured and estimated volume.

Measured *V* (ml)	Estimated *V* (ml)	Error	Relative Error (%)
175	188.199	13.199	7.542
100	92.355	−7.645	7.645
100	105.514	5.514	5.514
200	190.231	−9.769	4.885
100	108.416	8.416	8.416
100	101.176	1.176	1.176
275	272.805	−2.195	0.798
300	284.067	−15.933	5.311
250	243.155	−6.845	2.738
162.5	169.661	7.161	4.407

Average Relative Error (n = 287) = 4.527%.

Table 8
Comparison between measured and estimated mass.

Measured *M* (g)	Estimated *M* (g)	Error (g)	Relative Error (%)
152.1	156.7	4.6	3.024
156.7	181.9	25.2	16.082
262	276	14	5.344
120.3	121	0.7	0.582
181.9	156.7	−25.2	13.854
293.6	276	−17.6	5.995
152.1	162.7	10.6	6.969
156	152.1	- 4.6	2.936
368.7	363.1	- 5.6	1.519
265.4	262	- 3.4	1.281

Average Relative Error (n = 287) = 2.804%.

The D is the average distance between the boundary points and the center of gravity of an image. The radial distance is measured from the central point (centroid) in the object of each pixel $x(n)$, $y(n)$ on the boundary according to Eq. (9).

$$d(n) = \sqrt{[X(n) - \bar{X}]^2 + [Y(n) - \bar{Y}]^2} \qquad n = 0,1, \ldots, N-1 \tag{9}$$

2.4.2. 3D features

The volume (V) and surface area (S) were used as 3D features. These features were related to the volume of the tomato. The depth images acquired were used for these features that relate to the three-dimensional shape of the tomato. For the S, 3D Delaunay triangulation was used for approximation. The Delaunay triangulation creates a set of triangles in the 3D space. The total surface area was approximated by summing all areas of the triangles according to Eq. (10):

$$S = \sum_{i=1}^{T} \frac{1}{2} |x_i \times y_i| \tag{10}$$

where T is the total number of triangles, and $x_i$and y_i are the two vectors that span the ith triangle.

The V was estimated using numerical integration of the depth pixels using Eq. (11).

$$V = \sum_{i=1}^{N} (b - c_i) \cdot A_i \tag{11}$$

where V is the estimated volume, N is the total number of pixels, b is the average contour depth of the tomato, c_i is the depth value, and A_i is the approximated pixel area of the ith pixel.

2.5. Regression models

To predict the mass and volume of the tomatoes based on the extracted feature variables, five regression models were explored in this study, namely; Support vector machine (SVM) models (linear, quadratic, cubic, and radial basis function (RBF)) and Bayesian artificial neural network (Bayesian-ANN). SVM models have significant advantages over other supervised learning algorithms, and they offer the best accuracy (performance) on the training data, direct geometric interpretation, and elegant mathematical tractability. They also avoid overfitting of the data by not requiring a large number of training samples (Li et al., 2010). Bayesian optimization was used to tune the SVM classifier. The RBF-ANN model was implemented using the Neural Network Toolbox in MATLAB R2019a (The MathWorks Inc., Natick, MA, USA) software. The topologies consisting of inputs, hidden layers, and output were selected according to the feature groups they represent, as shown in Table 1. Bayesian regularization training algorithm was implemented, and the models were trained and retrained until there was a minimal error on the correlation between the output and the targets.

A 10-fold cross-validation-based parameter search trained all the models on the training dataset and subsequently evaluated on a testing dataset. For each variable to be predicted (mass or volume), three models were developed based on the feature variables used in training, i.e., a model of 2D features (*M1*), 3D features (*M2*) and a combination of 2D and 3D (*M3*). The model properties have been summarized in Table 1. For more insight on SVM and Bayesian-ANN, please refer to studies by (El Hariri et al., 2014a, 2014b; Wu and Zhou, 2006) and (Baltazar et al., 2008) respectively. The whole dataset consisted of 958 samples. For model evaluation, the samples were divided into two subsets, a training set of 671 samples (70%), and a test and validation set of 287 samples (30%). The data selection criteria were based on manual selection of images under the condition that the tomato does not touch the image edge due to the movement of the conveyor belt during image acquisition.

The RBF-SVM kernel parameters were computed iteratively during the 10-fold cross-validation in the model training phase. These classifier parameters affect the model performance by balancing between accuracy, overfitting, and underfitting to have a good generalization ability. In the Bayesian-ANN model development, the number of hidden layers was set to 10 after evaluation of the percent error during validation. However, as the number of neurons increases, percent error decreases while computation time increases (Hagan et al., 1996; Haykin, 1994).

2.6. Statistical analysis

A comprehensive descriptive analysis was performed on the

measured volume and mass dataset (n = 300). The statistical analyses were performed using the Microsoft Excel analysis toolpack option in office 2019 (Ms corporation, Redmond, WA). Additionally, to determine the relationship between cherry tomato volume and mass, a power function was fitted to mass and volume by a line fitting technique using the Curve Fitting Toolbox in Matlab R2019a (The Mathworks Inc., Natick, Ma, USA) software. The achieved power equation represented the regression model for mass estimation based on measured volume. The estimated mass was then compared against the real mass.

3. Results and discussion

3.1. The relation between tomato mass and volume measure

With reference to density-based packaging, this study investigated the relationship between the measured mass and measured volume. Of the total tomatoes used in the experiment, 250 were used to develop a power model of the measured M and measured V. Fig. 4(a) presents the scatter of mass against volume and Fig. 4(b) presents the scatter of predicted mass against measured mass. The evaluation established a power equation of $M = 1.312V^{0.9551}$ with an R^2 of 0.9751 (Fig. 4(a)) where M is the measured mass and V is the measured volume. Mass was then predicted based on the power model for 50 tomatoes and the results returned an R^2 of 0.9824 with an RMSE of 15.82g. From Table 2, the average relative error was 4.60%.

3.2. Models performance evaluation

The developed models (*M1, M2, and M3*) were evaluated on the testing dataset. Table 3 presents a summary of the performance of these models. The results indicated that generally, the models were accurate in prediction, although with some minor differences. From the results, it can be perceived that there was an alternating maximum accuracy between RBF-SVM and Bayesian-ANN in the explored models.

Furthermore, it can be observed that *M2* had the lowest accuracy in comparison to all the other models. In *M1*, RBF-SVM and Bayesian-ANN outperformed all the other models in *M* and *V* estimation, respectively. In *M2*, Bayesian-ANN outperformed all the other explored models in the prediction of both *M* and *V*. Lastly, in *M3*, Bayesian-ANN and RBF-SVM outperformed all the other models in the prediction of *M* and *V* respectively. Figs. 5 and 6 depicts the correlation of the predicted V and M with the measured V and M for all the models. This study aimed at establishing the difference in performance between the commonly used 2D and 3D image features. Therefore, the models developed were based on 2D, 3D, and a combination of both 2D and 3D feature variables for comparative analysis. Furthermore, the results for *M1* (only 2D features) concurred with those of UluiŞik et al. (2018) in tomato volume estimation based on ellipsoid estimation technique, Lee et al. (2006) in apples, strawberries, tomatoes, and cantaloupes volume estimation based on multiple silhouettes. Moreover, the application of Kinect RGB-depth sensor by Wang and Li (2014) estimated the volume of sweet onions by linear regression model (96.3%–97.9% accuracy) reported almost similar results compared to this study. Additionally, Yang et al. (2011) developed partial least squares regression (PLSR) and back-propagation artificial neural network (BPANN) for tomato size estimation based on visible and near-infrared (VIS-NIR) spectroscopy. The study reported a R^2 of 0.82 for the PLSR model and a R^2 of 0.88 for the PLS-BPANN model.

3.3. Statistical analysis of the dataset

Descriptive statistics of the dataset are presented in Table 4. Reviewing the data of the 300 tomato fruits suggested that the mean value of 249.04 g and 244.88 ml might not accurately reflect the actual mass and volume respectively of a tomato as larger masses and volume skewed the mean. Table 4 shows the median as 242.30 g and a positive skew of 0.38 for mass and a median of 231.00 g and a positive skew of 0.39 for volume indicating an axys-symmetrical distribution. The mean and median of measured mass had a rather slight variation compared to that of measured volume. Table 5 and 6 presents the performance of the two best models i.e. Bayesian-ANN and the RBF-SVM models.

3.4. Volume and mass estimation

Real-time measurement of tomato mass and volume is a time-consuming and tedious task. However, a volume-based sorting system is more economical and may provide a more effective and alternative method than mass sorting, as fruits are often graded and sorted according to size (Koc, 2007; Omid et al., 2010). If the fruit density is assumed to be constant, then one can readily estimate its mass from the volume (with any density variations being unpredictable and small) and vice versa, avoiding the need for a weighing device on the packing line. Volume can also be used to predict harvest time (Hahn and Sanchez, 2000).

The volume obtained using the WDM was compared with the volume determined by the two models used in this study. Table 7 presents a comparative analysis of measured *V* to the predicted *V* based on RBF-SVM for *M3* (highest accuracy). It can be observed that the maximum relative error was 8.416% while the minimum at 0.798% at an average of 4.53% on the entire testing dataset. Based on previous studies on volume and mass estimation of several fruits such as lemon, lime, orange, and tangerine the limit of agreement was set at 95%, such that the accepted estimated volume should be within 5% error (Omid et al., 2010). Additionally, Khojastehnazhand et al. (2010a); Koc (2007); Fellegari and Navid, 2011 determined tangerine volume, watermelon volume, and orange volume respectively using image processing. These three studies applied the *t*-test to compare volumes obtained using water displacement and image processing. These studies reported no significant difference between the two volumes in the 95% limits of agreement level ($P > 0.05$). Consequently, it can be concluded that the estimated volume for our study was within the acceptable error range. These errors mainly occurred due to inaccuracies in the WDM. Table 8 depicts a comparative analysis of the estimated *M* based on RBF-SVM for *M1* (highest accuracy) to the real *M*. it can be observed that the maximum and minimum relative errors were 16.082% and 0.582% respectively at an average of 2.80% on the entire testing dataset.

This proposed technique, achieved an average accuracy of 94% using RBF-SVM model and 95% using Bayesian-ANN model for volume estimation and 95% accuracy (on average) and 96% accuracy (on average) using RBF-SVM and Bayesian-ANN models respectively for mass estimation. This shows that this technique had better accuracy for mass prediction and almost similar results for volume estimation in comparison to other studies. It can also be concluded that based on computer vision technique for *M* estimation, 2D image features would be the most preferred while for *V*, a combination of both 2D and 3D image feature variables would be most preferred as predictors. Moreover, tomato *M* and *V* are linearly positively correlated, and this can be used as a representation of tomato fruit density in density-based sorting.

4. Conclusion

The focus of this research was to develop a novel computer vision system for tomato volume and mass estimation. The relation between mass and volume was explored for density-based packages of cherry tomatoes, under which mass was estimated at an R^2 of 0.9824, least accuracy of 0.9226 and the highest accuracy of 0.9706 based on a developed power equation model relating mass and volume. Furthermore, the success and accuracy of an automatic computer vision sorting system depend on the quality of the image. Thus, this study was based on depth images for both 2D and 3D image analysis. Correlation models

were then developed to estimate mass and volume with different image predictors (2D,3D, and a combination of 2D and 3D). However, this study had some limitations; the mass/volume relationship reported can only be applied to cherry tomatoes variety used in this study. With other tomato fruit types, especially the ones with big fruits, the volume/mass relationships are different than the cherry fruits as the internal fruit structure (locule number and flesh percentage) could have significant differences.

Consequently, these relationships need to be determined for each tomato type. Therefore, this system needs to be validated on different varieties of tomatoes for potential application in volume and mass estimation of other axys-symmetric fruits and vegetables. A stronger contrast of its reproducibility is needed using fruits from different seasons and localities or markets in order to determine its preciseness. This is due to the regression techniques used that tends to adapt to the data used in model development; this usually brings useful data to fit parameters but could limit its general use. For real in-line use, more extensive data sources must be used to develop the prediction models.

Moreover, the mass prediction results from volume data are based on the premise that cherry fruit density is constant. This is not always true as the growing system used can significantly affect the cherry fruit density as showed by Stertz et al. (2005) when evaluated the effects of conventional, organic, and hydroponic growing system in several morphological traits of cherry fruits. So, the results obtained will be referred only to the class of the fruits studied. Despite these limitations, this study achieved its objective by having acceptable accuracies on the testing dataset. Thus, this system as a non-destructive technique can be applied in both online and inline post-harvest processing of tomatoes for automatic sorting and grading procedures as the identification of fruit size will improve the packaging-process by increasing the uniformity of the packaging.

Conflicts of interest

All authors declare that they have no conflict of interest.

Acknowledgments

All experiments were carried out in Nanjing Agricultural University facilities, in compliance with and using protocols approved by the Biosafety committee of Nanjing Agricultural University in the handling of agricultural food. The authors appreciate the support and financial assistance under Jiangsu Agricultural Science and Technology Innovation Fund CX-(17)1003, provided by the College of Engineering, Nanjing Agricultural University, China.

References

Andersen, M., Jensen, T., Lisouski, P., Mortensen, A., Hansen, M., Gregersen, T., Ahrendt, P.J.A.U., 2012. Kinect Depth Sensor Evaluation for Computer Vision Applications. pp. 1–37.

Arendse, E., Fawole, O.A., Magwaza, L.S., Opara, U.L., 2018. Non-destructive prediction of internal and external quality attributes of fruit with thick rind: A review. J. Food Eng. 217, 11–23. https://doi.org/10.1016/j.jfoodeng.2017.08.009.

Baltazar, A., Aranda, J.I., Gonzalez-Aguilar, G., 2008. Bayesian classification of ripening stages of tomato fruit using acoustic impact and colorimeter sensor data. Comput. Electron. Agric. 60 (2). https://doi.org/10.1016/j.compag.2007.07.005.

Chang, C.H., Lin, H.Y., Chang, C.Y., Liu, Y.C., 2006. Comparisons on the antioxidant properties of fresh, freeze-dried and hot-air-dried tomatoes. J. Food Eng. 77 (3). https://doi.org/10.1016/jfoodeng.2005.06.061.

Chen, Y.R., Chao, K.L., Kim, M.S., 2002. Machine vision technology for agricultural applications. Comput. Electron. Agric. 36 (2–3), 173–191. https://doi.org/10.1016/S0168-1699(02)00100-X.

Chopin, J., Laga, H., Miklavcic, S.J., 2017. A new method for accurate, high-throughput volume estimation from three 2D projective images. Int. J. Food Prop. 20 (10). https://doi.org/10.1080/10942912.2016.1236814.

Concha-Meyer, A., Eifert, J., Wang, H., Sanglay, G., 2018. Volume estimation of strawberries, mushrooms, and tomatoes with a machine vision system. Int. J. Food Prop. 21 (1), 1867–1874. https://doi.org/10.1080/10942912.2018.1508156.

Corti, A., Giancola, S., Mainetti, G., Sala, R., 2016. A metrological characterization of the Kinect V2 time-of-flight camera. Robot. Auton. Syst. 75, 584–594. https://doi.org/10.1016/j.robot.2015.09.024.

Costa, C., Antonucci, F., Pallottino, F., Aguzzi, J., Sun, D.-W., Menesatti, P.J.F., Technology, B., 2011. Shape analysis of agricultural products: A review of recent research advances and potential application to computer vision. Food Bioprocess Technol. 4 (5), 673–692.

Ireri, David, Cedric, O., Li, Jiawei, Changying, J.I., 2018. An Implementation of a low-cost tomato sorter by A Monochromatic camera and arduino. In: International Journal of Emerging Technology and Advanced Engineering. 8 2.

Du, C.J., Sun, D.W., 2006a. Estimating the surface area and volume of ellipsoidal ham using computer vision. J. Food Eng. 73 (3), 260–268. https://doi.org/10.1016/j.jfoodeng.2005.01.029.

Du, C.J., Sun, D.W., 2006b. Learning techniques used in computer vision for food quality evaluation: A review. J. Food Eng. 72 (1), 39–55. 10.1016. https://doi.org/10.1016/j.jfoodeng.2004.11.017.

Duzyaman, E., Duzyaman, B.U., 2005. Fine-tuned head weight estimation in globe artichoke (Cynara scolymus L.). Hortscience 40 (3), 525–528. https://doi.org/10.21273/HORTSCI.40.3.525.

Ehsani, R., Toudeshki, A., Wan, P.J.T.P., 2016. New sensor technology for yield estimation and disease detection. Tomato Proc 15–16 Retrieved from. https://swfrec.ifas.ufl.edu/docs/pdf/veg-hort/tomato-institute/presentations/ti2016/ti2016_Ehsani.pdf.

Eifert, J.D., Sanglay, G.C., Lee, D.-J., Sumner, S.S., Pierson, M.D., 2006. Prediction of raw produce surface area from weight measurement. J. Food Eng. 74 (4), 552–556. https://doi.org/10.1016/j.jfoodeng.2005.02.030.

El-Bendary, N., El Hariri, E., Hassanien, A.E., Badr, A., 2015. Using machine learning techniques for evaluating tomato ripeness. Expert Syst. Appl. 42 (4), 1892–1905. https://doi.org/10.1016/j.eswa.2014.09.057.

El Hariri, E., El-Bendary, N., Hassanien, A.E., Badr, A., 2014a. Automated ripeness assessment system of tomatoes using pca and svm techniques, *Computer vision and image processing in intelligent systems and multimedia technologies*. IGI global 101–130. https://doi.org/10.4018/978-1-4666-6030-4.ch006.

El Hariri, E., El-Bendary, N., Fouad, M.M.M., Platoš, J., Hassanien, A.E., Hussein, A.M., 2014b. Multi-class SVM Based Classification Approach for Tomato Ripeness, *Innovations in Bio-Inspired Computing and Applications*. Springer, pp. 175–186. https://doi.org/10.1007/978-3-319-01781-5_17.

FAOSTAT, 2017. Food and Agriculture Organization (FAO), Statistics, 2017 ed. . http://www.fao.org/faostat/en.

Fellegari, R., Navid, H., 2011. Determining the orange volume using image processing. International Confrence on Food Engineering and Biotechnology 9. http://ipcbee.com/vol9/34-B10018.pdf, Accessed date: 15 July 2019.

Gonzalez-Jorge, H., Rodríguez-Gonzálvez, P., Martínez-Sánchez, J., González-Aguilera, D., Arias, P., Gesto, M., Díaz-Vilariño, L., 2015. Metrological comparison between Kinect I and Kinect II sensors. Measurement 70, 21–26. https://doi.org/10.1016/j.measurement.2015.03.042.

Gül, S., Özdemir, A., 2017. Smartphone Controlled Ultrasonic Nondestructive Testing System Design. International Conference on Engineering Technologies, Konya, Türkiye, pp. 335–338.

Hagan, M.T., Demuth, H.B., Beale, M.H., De Jesús, O., 1996. Neural Network Design. Pws Pub, Boston.

Hahn, F., Sanchez, S., 2000. Carrot volume evaluation using imaging algorithms. J. Agric. Eng. Res. 75 (3), 243–249. https://doi.org/10.1006/jaer.1999.0466.

Haykin, S., 1994. Neural Networks: A Comprehensive Foundation. Prentice Hall PTR.

Ioana, R., Ardelean, M., Mitre, V., Hârşan, 2007. Phenotypic, genotypic and environmental correlations between fruit characteristics confirming suitability to juice extraction in winter apple. Bull. Univ. Agric. Sci. Vet. Med. Cluj-Napoca - Hortic. 64 (1/2), 58–62.

Iqbal, S.M., Gopal, A., Sarma, A., 2011. Volume estimation of apple fruits using image processing, *Image Information Processing (ICIIP)*. In: 2011 International Conference on. IEEE, pp. 1–6.

Jadhav, T., Singh, K., Abhyankar, A.J.M.T., Applications, 2019. Volumetric Estimation Using 3D Reconstruction Method for Grading of Fruits. pp. 1–22. https://doi.org/10.1007/s11042-018-6271-3.

Jana, A., 2012. Kinect for Windows SDK Programming Guide. Packt Pub.

Khojastehnazhand, M., Omid, M., Tabatabaeefar, 2010a. Determination of tangerine volume using image processing methods. Int. J. Food Prop. 13 (4), 760–770. https://doi.org/10.1080/10942910902894062.

Khojastehnazhand, M., Omid, M., Tabatabaeefar, A., 2010b. Development of a lemon sorting system based on color and size. Afr. J. Plant Sci. 4 (4), 122–127. Retrieved from. http://www.academicjournals.org/app/webroot/article/article1380110185_Khojastehnazhand%20et%20al.pdf.

Koc, A.B.J., 2007. Determination of watermelon volume using ellipsoid approximation and image processing. Postharvest Biol. Technol. 45 (3), 366–371. https://doi.org/10.1016/j.postharvbio.2 007.03.010.

Kumar, K., Paswan, S., Srivastava, S., 2012. Tomato-a natural Medicine and its health benefits. J. Pharmacogn. Phytochem. 1 (1). https://doi.org/10.22271/phyto.

Lee, D.J., Eifert, J.D., Westover, B.P., 2002. Surface Area and Volume Measurement Using Radial Projections, Vision Geometry XI. International Society for Optics and Photonics, pp. 92–101. https://doi.org/10.1117/12.452358.

Lee, D.J., Xu, X.Q., Eifert, J., Zhan, P.C., 2006. Area and volume measurements of objects with irregular shapes using multiple silhouettes. Opt. Eng. 45 (2), 027202. https://doi.org/10.1117/1.2166847.

Li, D., Yang, W., Wang, S., 2010. Classification of foreign fibers in cotton lint using machine vision and multi-class support vector machine. Comput. Electron. Agric. 74 (2), 274–279. https://doi.org/10.1016/j.compag.2010.09.002.

Li, Q., Wang, M., Gu, W.J.C., 2002. Computer vision based system for apple surface defect detection. Comput. Electron. Agric. 36 (2–3), 215–223. https://doi.org/10.1016/

S0168-1699(02)00093-5.
Mathiassen, J.R., Misimi, E., Toldnes, B., Bondø, M., Østvik, S.O., 2011. High-speed weight estimation of whole herring (Clupea harengus) using 3D machine vision. J. Food Sci. 76 (6), E458–E464. https://doi.org/10.1111/j.1750-3841.2011.02226.x.
Mohsenin, N.N., 1970. Physical properties of plant and animal materials. Structure, Physical Characteristics and Mechanical Properties 1, vol. 1 Gordon & Breach Science Publishers Inc, New York, USA.
Moreda, G., Ortiz-Cañavate, J., García-Ramos, F.J., Ruiz-Altisent, M.J., 2009. Non-destructive technologies for fruit and vegetable size determination–a review. J. Food Eng. 92 (2), 119–136. https://doi.org/10.1016/j.jfoodeng.2008.11.004.
Morrey Jr., C.B., 2009. Multiple Integrals in the Calculus of Variations. Springer Science & Business Media.
Naik, S., Patel, B., 2017. Machine vision based fruit classification and grading-A review. Int. J. Comput. Appl. 170 (9), 22–34. Retrieved from. https://pdfs.semanticscholar.org/4aa0/a0cdfe036b512b9c6a0e9f34c7f47382a27d.pdf.
Nguyen, T.-N., Huynh, H.-H., Meunier, J.J.I.A., 2018. 3d reconstruction with time-of-flight depth camera and multiple mirrors. 6. pp. 38106–38114.
Okinda, C., Lu, M., Nyalala, I., Li, J., Shen, M., 2018. Asphyxia occurrence detection in sows during the farrowing phase by inter-birth interval evaluation. Comput. Electron. Agric. 152, 221–232. https://doi.org/10.1016/j.compag.2018.07.007.
Omid, M., Khojastehnazhand, M., Tabatabaeefar, A., 2010. Estimating volume and mass of citrus fruits by image processing technique. J. Food Eng. 100 (2), 315–321. https://doi.org/10.1016/j.jfoodeng.2010.04.015.
Otsu, N., 1979. A threshold selection method from gray-level histograms. IEEE Trans. Syst. Man Cyber. 9 (1), 62–66. Retrieved from. https://pdfs.semanticscholar.org/fa29/610048ae3f0ec13810979d0f27ad6971bdbf.pdf.
Rashidi, M., Gholami, M.J., 2008. Determination of kiwifruit volume using ellipsoid approximation and image-processing methods. Int. J. Agric. Biol. 10 (4), 375–380.
Rizzolo, A., Vanoli, M., Spinelli, L., Torricelli, A., 2010. Sensory characteristics, quality and optical properties measured by time-resolved reflectance spectroscopy in stored apples. Postharvest Biol. Technol. 58 (1), 1–12. https://doi.org/10.1016/j.postharvbio.2010.05.003.
Saad, A.M., Ibrahim, A., El-Bialee, N., 2016. Internal quality assessment of tomato fruits using image color analysis. Agric. Eng. Int.: CIGR J. 18 (1), 339–352.
Sabliov, C., Boldor, D., Keener, K., Farkas, B., 2002. Image processing method to determine surface area and volume of axi-symmetric agricultural products. Int. J. Food Prop. 5 (3), 641–653. https://doi.org/10.1081/JFP-120015498.
Satpute, M.R., Jagdale, S., 2016. Color, size, volume, shape and texture feature extraction techniques for fruits: A review. Int. Res. J. Eng. Technol. 3, 703–708 3(02).
Schulze, K., Nagle, M., Spreer, W., Mahayothee, B., Müller, J., 2015. Development and assessment of different modeling approaches for size-mass estimation of mango fruits (Mangifera indica L., cv.'Nam Dokmai'). Comput. Electron. Agric. 114, 269–276. https://doi.org/10.1016/j.compag.2015.04.013.
Semary, N.A., Tharwat, A., Elhariri, E., Hassanien, A.E., 2015. Fruit-based tomato grading system using features fusion and support vector machine. Springer, pp. 401–410. Advances in Intelligent Systems and ComputingIntelligent Systems' 2014. https://doi.org/10.1007/978-3-319-11310-4_35.
Siswantoro, J., Prabuwono, A.S., Abdulah, A., 2013. Volume measurement of food product with irregular shape using computer vision and Monte Carlo method: A framework. In: 4th International Conference on Electrical Engineering and Informatics (Iceei 2013). Proc. Technol. 11. pp. 764–770. https://doi.org/10.1016/j.protcy.2013.12.256.
Stertz, S.C., Espírito Santo, A.P.d., Bona, C., Freitas, R.J.S.d., 2005. Comparative morphological analysis of cherry tomato fruits from three cropping systems. Sci. Agric. 62 (3), 296–298. https://doi.org/10.1590/S0103-90162005000300015.
Takeoka, G.R., Dao, L., Flessa, S., Gillespie, D.M., Jewell, W.T., Huebner, B., Bertow, D., Ebeler, S.E., 2001. Processing effects on lycopene content and antioxidant activity of tomatoes. J. Agric. Food Chem. 49 (8), 3713–3717. https://doi.org/10.1021/jf0102721.
UluiŞik, S., Yildiz, F., ÖzdemİR, A.T., 2018. Image Processing Based Machine Vision System for Tomato Volume Estimation, *2018 Electric Electronics. Computer Science, Biomedical Engineerings' Meeting (EBBT)*. IEEE, pp. 1–4. https://doi.org/10.1109/EBBT.2018.8391460.
Van de Poel, B., Bulens, I., Hertog, M., Van Gastel, L., De Proft, M., Nicolai, B., Geeraerd, A., 2012. Model-based classification of tomato fruit development and ripening related to physiological maturity. Postharvest Biol tec 67, 59–67. https://doi.org/10.1016/j.postharvbio.2011.12.005.
Vivek Venkatesh, G., Iqbal, S.M., Gopal, A., Ganesan, D., 2015. Estimation of volume and mass of axi-symmetric fruits using image processing technique. Int. J. Food Prop. 18 (3), 608–626. https://doi.org/10.1080/10942912.2013.831444.
Wan, P., Toudeshki, A., Tan, H.Q., Ehsani, R., 2018. A methodology for fresh tomato maturity detection using computer vision. Comput. Electron. Agric. 146, 43–50. https://doi.org/10.1016/j.compag.2018.01.011.
Wang, D., Martynenko, A., Corscadden, K., He, Q.J., 2017. Computer vision for bulk volume estimation of apple slices during drying. Dry. Technol. 35 (5), 616–624. https://doi.org/10.1080/07373937.2016.1196700.
Wang, T.Y., Nguang, S.K., 2007. Low cost sensor for volume and surface area computation of axi-symmetric agricultural products. J. Food Eng. 79 (3), 870–877. https://doi.org/10.1016/j.jfoodeng.2006.01.084.
Wang, W., Li, C., 2014. Size estimation of sweet onions using consumer-grade RGB-depth sensor. J. Food Eng. 142, 153–162. https://doi.org/10.1016/j.jfoodeng.2014.06.019.
Wei, Y.Y., Xu, M., Wu, H.L., Tu, S.C., Pan, L.Q., Tu, K., 2016. Defense response of cherry tomato at different maturity stages to combined treatment of hot air and Cryptococcus laurentii. Postharvest Biol tec 117, 177–186. https://doi.org/10.1016/j.postharvbio.2016.03.001.
Wu, Q.A., Zhou, D.X., 2006. Analysis of support vector machine classification. J. Comput. Anal. Appl. 8 (2), 99–119.
Yang, H.Q., Kuang, B.Y., Mouazen, A.M., 2011. Size Estimation of Tomato Fruits Based on Spectroscopic Analysis, *Advanced Materials Research*. Trans Tech Publ, pp. 1254–1257. https://doi.org/10.4028/www.scientific.net/AMR.225-226.1254.
Ziaratban, A., Azadbakht, M., Ghasemnezhad, A., 2017. Modeling of volume and surface area of apple from their geometric characteristics and artificial neural network. Int. J. Food Prop. 20 (4), 762–768. https://doi.org/10.1080/10942912.2016.1180533.